Radiophysics and Quantum Electronics, Vol. 54, No. 6, November, 2011
(Russian Original Vol. 54, No. 6, June, 2011)

INFLUENCE OF THE AXIAL MISALIGNMENT OF THE ELECTRON BEAM AND THE CAVITY ON THE GYROTRON PARAMETERS

N. A. Zavol'skiy, V. E. Zapevalov,* M. A. Moiseev, and A. S. Sedov

UDC 533.86

We consider some effects connected with the axial misalignment of the electron beam and the cavity in gyrotrons. These effects are studied by the example of three gyrotrons with different parameters of the electron beam and output characteristics. The experimental data and the results of computer calculations are compared on the basis of a multi-mode nonstationary model of the electron-wave interaction in the gyrotron cavity.

1. INTRODUCTION

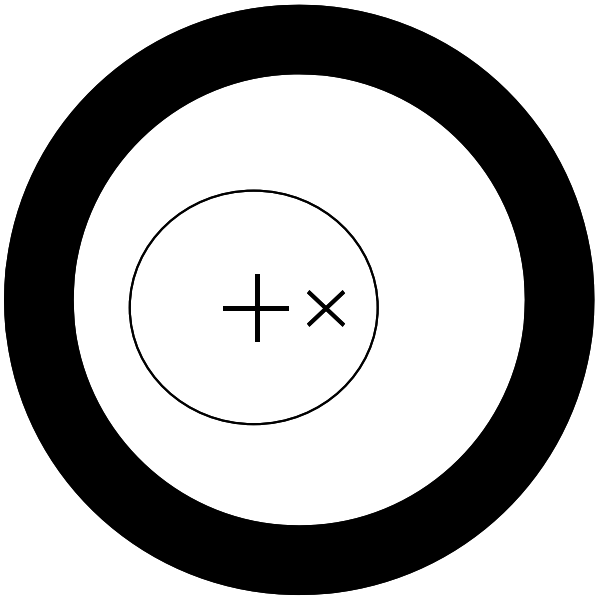

Fig. 1. Scheme of the axial misalignment of the beam and the cavity: the times sign and the cross mark the cavity axis and the beam axis, respectively.

Many reasons, such as technological errors of gyrotron manufacture or poor adjustment of the magnetic field of the solenoid, can result in the formation of the so-called axial misalignment, i.e., the situation where the axis of the guiding centers of the electron beam does not coincide with the cavity axis (see Fig. 1 and [1]). In this case, phenomena, which are connected with the violation of the axial symmetry in the resonator—beam system, may arise. As operating frequencies of the gyrotron increase and, correspondingly, the working wavelengths decrease, this problem becomes more and more acute and actually inevitable. Earlier, the problems discussed in literature were mainly related to the decrease of the coupling between the working mode and the beam which results in a decrease in the tube efficiency [2, 3]. However, it is also of interest to study the phenomena which are due to an increase in the coupling of the beam and some spurious mode. In this case, the two-mode generation regime can be realized. A specific case of such a regime is the generation of counter-rotating modes with comparable amplitudes at the same frequency, i.e., the formation of a standing wave.

This paper considers the effects connected with the axial misalignment of the electron beam in three gyrotrons having different parameters and operated in the continuous-wave (CW) regime. In this case, one can analyze what specific effects casued by the axial misalignment are typical of a gyrotron with certain parameters. All these gyrotrons have simple electrodynamic systems in the form of a regular circular cavity, an input subcritical narrowing, and an output widening.

* zapev@appl.sci-nnov.ru

Institute of Applied Physics of the Russian Academy of Sciences, Nizhny Novgorod, Russia. Translated from Izvestiya Vysshikh Uchebnykh Zavedenii, Radiofizika, Vol. 54, No. 6, pp. 444–450, June 2011. Original article submitted January 18, 2011; accepted June 28, 2011.

TABLE 1.

	Power 1 MW, operating frequency 170 GHz	Power 3 kW, operating frequency 300 GHz	Power 200 W, operating frequency 258 GHz
Working mode	$TE_{25,10}$	$TE_{22,8}$	$TE_{-2,3}$
Harmonic number	1	1	2
Accelerating voltage, kV	80	15	14
Beam current, A	35	1	0.4
Cavity radius, mm	17.785	8.39	1.84
Beam radius, mm	7.4	3.71	0.981
Pitch factor	1.2	1.0	1.3
Spread of transverse velocities	0.3	0.3	0.3

The code used for numerical simulation was based on the multimode nonstationary model of the electron-wave interaction in a gyrotron with the self-consistent non-fixed structure of the high-frequency field [4, 5], which was generalized to the case of misalignment of the beam and the cavity. The parameters of the electron beam, which were used in the calculations, corresponded to the typical experimental values, as well as the results of the electron-optical measurements and calculations. Within the considered model, the beam was assumed to be infinitely thin and symmetric with respect to its own axis, and the beam current density, distributed uniformly over the azimuth.

The main parameters of the gyrotrons under consideration are given in Table 1. When performing the numerical simulation, we assumed that the parameters of the electron beam are independent of its axial misalignment with the cavity.

The average radius R_0 of the beam in the cavity is usually chosen such as to ensure the maximum coupling of the electron beam and the working mode and weakened coupling with spurious modes. The above-said coupling for the case of an axially aligned beam is determined by the value of the structural factor

$$G_{mp} = \frac{J^2_{m-n}(\nu_{mp} R_0/R_\mathrm{p})}{J^2_m(\nu_{mp})\,(\nu^2_{mp} - m^2)}, \tag{1}$$

where n is the number of the working cyclotron-frequency harmonic, $J_m(x)$ is the Bessel function, ν_{mp} is the root of the equation $J'_m(\nu_{mp}) = 0$, R_0 is the radial coordinate of the centers of the electron orbits, and R_p is the radius of the cylindrical part of the cavity.

It seems necessary to evaluate the permissible value of the axial misalignment, at which its negative influence is still admissible, and to study the effects that arise when this value is exceeded.

2. GYROTRON WITH AN OUTPUT RADIATION FREQUENCY OF 170 GHz FOR CONTROLLED-FUSION APPLICATIONS

The first considered device is the gyrotron with an output radiation frequency of 170 GHz, which is operated in the continuous-wave regime at the first gyrofrequency harmonic and a megawatt power level. This gyrotron is used for electron-cyclotron plasma heating in the ITER tokamak [6, 7]. The version chosen for the numerical simulation was that developed at the Institute of Applied Physics of the Russian Academy of Sciences (IAP RAS) and the Research and Production Enterprise "GYCOM" and currently tested at Kurchatov Institute (Moscow, Russia) [8]. The numerical simulation considered the nonstationary four-wave interaction of the following modes: working mode $TE_{25,10}$, the adjacent spurious $TE_{22,11}$ mode, and counter-rotating $TE_{-25,10}$ and $TE_{-22,11}$ modes. The dependencies of the structural factors of these modes on the value d_R of the axial beam misalignment are shown in Fig. 2.

Figure 3 shows the dependencies of the partial efficiencies of the four above-specified modes in the

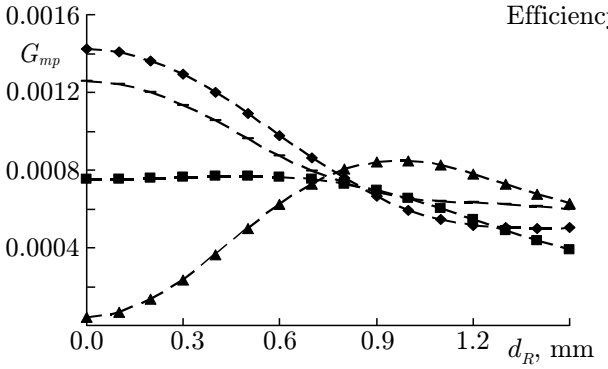

Fig. 2. Structural factors of the working mode $TE_{25,10}$ (♦), main spurious mode $TE_{22,11}$ (▲) and counter-rotating $TE_{-25,10}$ (■) and $TE_{-22,11}$ (−) modes.

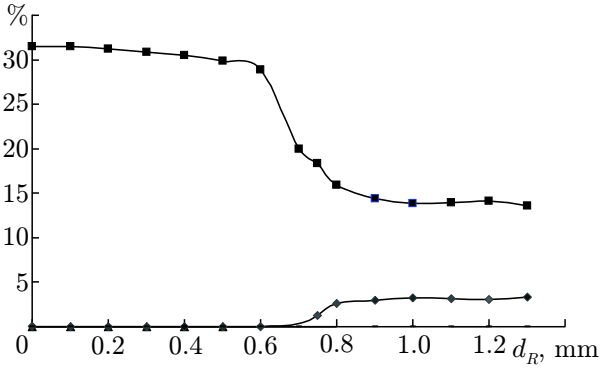

Fig. 3. Calculated partial efficiency for the $TE_{25,10}$ (■) and $TE_{22,11}$ (♦) modes as a function of the axial misalignment value for the gyrotron with an output radiation frequency of 170 GHz, accelerating voltage $U = 80$ kV, beam current $I = 35$ A, and magnetic field at the cavity center $B = 6.8$, which works at the first gyroharmonics.

steady state on the value d_R of the axial beam misalignment. The initial amplitudes of all the modes were assumed close to the stationary amplitude of the working mode. One can see in this Figure that as the axial misalignment increases up to 0.6 mm, i.e., 1/3 of the wavelength, the working mode suppresses the other modes, and the generation is single-mode. However, the efficiency decreases by almost 5% compared with the maximum value. As the axial misalignment further increases, the total efficiency drops rather sharply, and two modes are involved in the generation, specifically, $TE_{25,10}$ and $TE_{22,11}$. For the counter-rotating modes, efficiency values are negligibly small, and their generation was not observed during gyrotron tests [8].

3. GYROTRON WITH AN OUTPUT FREQUENCY OF 300 GHz OPERATED AT THE FIRST CYCLOTRON HARMONIC

The second considered gyrotron is operated in the continuous-wave regime at the first cyclotron harmonic with an output radiation frequency of 300 GHz. It was designed and manufactured at IAP RAS and GYCOM for the Research Center for Development of Far-Infrared Region, University of Fukui, Japan [9], where it was used in the experimental facility for a study of new materials, as well in biological and medical applications. The calculated radiation power of this gyrotron was 3.5 kW for an accelerating voltage of 15 kV, an electron beam current of up to 1 A, and a pitch factor of 1.2. However, experimental research showed that the maximum power level ranges from 1.6 to 2.3 kW [9, 10]. The power became limited when the two-frequency generation regime with close frequencies settled in. A most probable reason for this mismatch could be the misalignment of the electron beam and the cavity.

At the first stage of research, we performed computer simulation using the single-mode approximation. It showed that the decrease of the theoretical efficiency by 1.5–2 times, which was observed in the experiment, corresponded to the beam misalignment being 0.4–0.5 mm (see Fig. 4). The next stage was a simulation allowing for all the modes that could be excited in the generation zone. The time dependencies of the amplitudes of these modes for a misalignment of 0.5 mm are shown in Fig. 5. As in the above-considered gyrotron with an output radiation frequency of 170 GHz and a power of 1 MW, here a spurious mode is excited with high efficiency along with the working mode. For the counter-rotating modes, efficiency values are insignificant. The total output power of all generated modes corresponds to the experimental data and is equal to 1.7 kW. It also follows from the calculations that a two-frequency generation is possible, which agrees with the experimental results. It should be noted that the hysteresis effect was observed during numerical simulations starting at a certain value of the misalignment, i.e., two stable equilibrium states

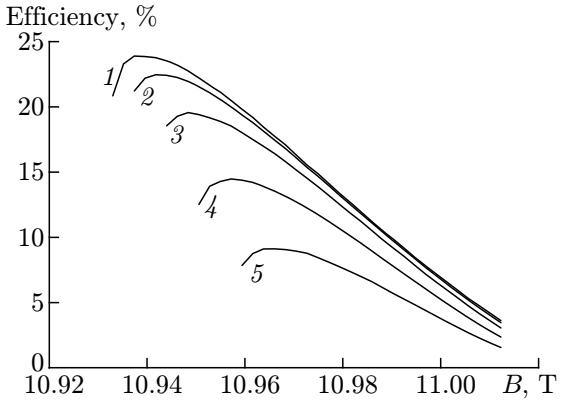

Fig. 4. dependencies of the working-mode efficiency on the magnetic field for different values d_R of the beam misalignment in the gyrotron with an output radiation frequency of 300 GHz: $d_R = 0.1$ mm (*1*), $d_R = 0.2$ mm (*2*), $d_R = 0.3$ mm (*3*), $d_R = 0.4$ mm (*4*), and $d_R = 0.5$ mm (*5*).

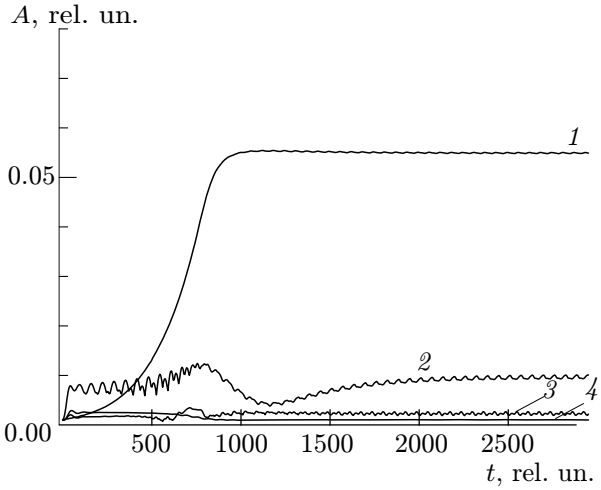

Fig. 5. Nonstationary mode interaction in the gyrotron with an output radiation frequency of 300 GHz for a beam misalignment of 0.5 mm. Conditional time units are plotted along the x axis (one unit corresponds to 25 ns). Wave amplitudes in relative units are plotted along the y axis for the $TE_{-22,8}$ mode (*1*), $TE_{22,8}$ mode (*2*), $TE_{-19,9}$ mode (*3*), and $TE_{19,9}$ mode (*4*); $U = 15$ kV, $I = 1$ A, $g = 1.2$, and $B = 10.9638$ T.

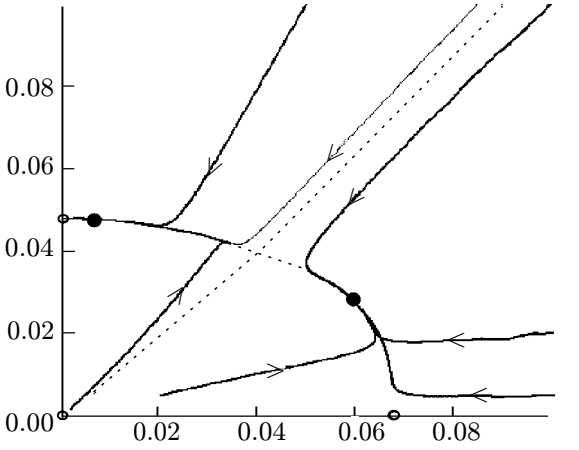

Fig. 6. Phase plane which explains the hysteresis effect for an electron beam misalignment of 0.5 mm. The amplitudes of the modes $TE_{22,8}$ and $TE_{-22,8}$ are plotted along the x axis and y axis, respectively, in relative units.

with approximately equal total radiation powers existed on the phase plane of the amplitudes of $TE_{22,8}$ and $TE_{-22,8}$ (see Fig. 6).

4. CW GYROTRON WITH AN OUTPUT RADIATION FREQUENCY OF 258 GHz AND A POWER OF 200 W OPERATED AT THE SECOND CYCLOTRON HARMONIC

The authors of [11-13] considered the issues of designing and optimizing a high-stability gyrotron with an output frequency of 258 GHz to be operated in the continuous-wave regime at the second gyrotron-frequency harmonic. This tube is currently a component of the dynamic nuclear polarization complex for magnetoresonance spectroscopy studies at the Institut für Biophysikalische Chemie, Goethe Universität, Frankfurt-am-Main, Germany. In the experiments [14], the specified level of parameters was achieved at the working mode, their high stability was demonstrated, and some spurious modes were observed.

However, two significant mismatches between the experimental data and the results of the preliminary numerical simulation were found, specifically:

1) the working $TE_{2,3}$ mode (as well as the spurious $TE_{4,2}$ mode) at the gyrotron window output had

the standing-wave structure in the azimuthal direction, i.e., it was a superposition of the counter-rotating $TE_{2,3}$ and $TE_{-2,3}$ waves with comparable amplitudes;

2) the $TE_{0,3}$ mode, which was generated as the guiding magnetic field increased by 2%, had a sufficiently high power of 100–150 W, although theoretically the starting conditions were not fulfilled since its starting current exceeded the operating current by approximately 7 times for the calculated parameters.

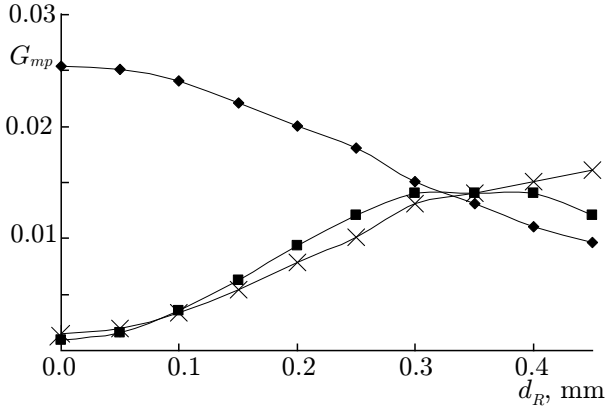

Fig. 7. Dependencies of the factors G_{mp} for the modes $TE_{2,3}$ (■), $TE_{-2,3}$ (♦), and $TE_{0,3}$ (×) on the misalignment of the electron beam and the cavity for the gyrotron with an output frequency of 258 GHz operated at the second cyclotron-frequency harmonic.

These effects could be explained by various deviations of the electron beam parameters from their theoretical values, specifically, its coaxial misalignment. Figure 7 shows the dependencies of the so-called G_{mp} factors, which determine the coupling between the mode and the beam, on the value of the electron beam misalignment for the modes $TE_{2,3}$, $TE_{-2,3}$, and $TE_{0,3}$. The values of d_R that exceeded 0.5 mm were not considered, since, allowing for the beam blurring and spurious emission out of the emitting cathode belt, such a beam would come in touch with the wall of the electrodynamic system. One can see in Fig. 7 that a misalignment of about 0.3–0.4 mm can result in both the combined generation of the $TE_{2,3}$ and $TE_{-2,3}$ modes and the generation of the symmetric $TE_{0,3}$ mode with a comparable power level. The numerical simulation confirmed this hypothesis.

Figure 8 shows the results of simulating the interaction of the $TE_{2,3}$ and $TE_{-2,3}$ modes, i.e., partial efficiencies of these modes in the stabilized state, as well as the total output efficiency as a function of the misalignment value. Figure 9 shows the efficiency of the $TE_{0,3}$ mode as a function of this value. One can see that for the misalignment ranging from 0.3 mm to 0.4 mm, the stabilization of the two-mode generation of the $TE_{2,3}$ and $TE_{-2,3}$ modes is accompanied (in the case of a different tuning of the magnetic field) by the generation of the $TE_{0,3}$ mode, and the output power in both cases are approximately equal and agree well with the experimental data. The technological errors and misalignment of the magnetic field and the cavity for a misalignment of 0.3–0.4 mm seem to be exceedingly great. However, it is impossible to check the deformations inside the tube caused by the thermal processes during its manufacture without damaging the tube.

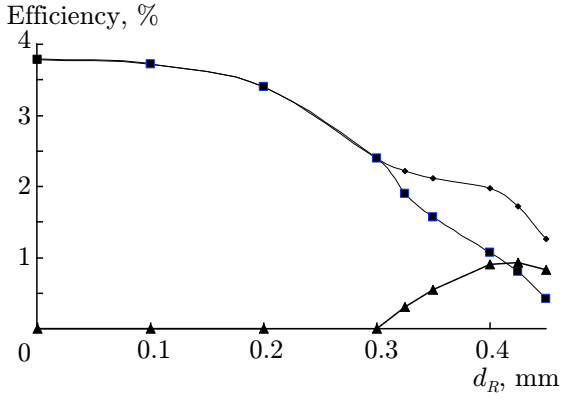

Fig. 8. Calculated partial efficiency for the modes $TE_{-2,3}$ (■) and $TE_{2,3}$ (▲) and the total efficiency (•) for the gyrotron with an output frequency of 258 GHz operated at the second gyrotron-frequency harmonic.

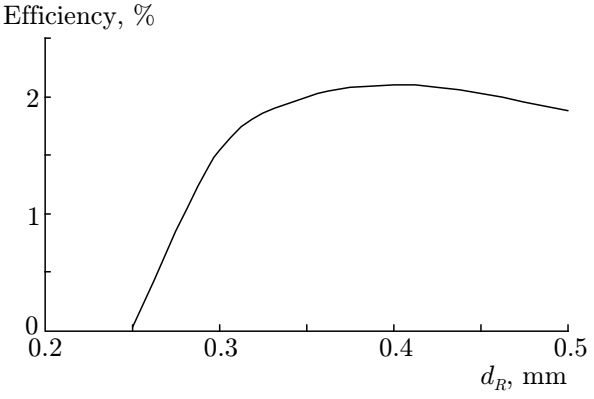

Fig. 9. Calculated efficiency for the $TE_{0,3}$ mode for the gyrotron with an output frequency of 258 GHz operated at the second cyclotron harmonic.

Thus, the results of the experiment can be explained by the axial misalignment of the electron beam and the cavity. Analytical and numerical studies of different models of gyrotrons [15] and other axisymmetric self-oscillating systems, specifically, ring-shaped lines with distributed nonlinear parameters [16], demonstrate the possibility of exciting only rotating modes. It is necessary to note that according to [17], the effect of the two-mode generation of the $TE_{2,3}$ and $TE_{-2,3}$ modes can be caused by a negligible deformation of the cavity wall for the amplitude of the fourth spatial harmonic, which is about 1 μm. The combined action of the above-mentioned factors seems to be the most probable reason.

5. CONCLUSIONS

The effects related to axial misalignment of the electron beam and the cavity have been studied for three gyrotrons operated in the continuous-wave regime. It is shown that the main effect for gyrotrons operated at comparatively high modes is the transition to the two-mode generation of the working mode and one of the spurious modes. For gyrotrons operated at relatively low modes, axial misalignment results in the formation of a standing wave (in the azimuthal direction). In both cases, one can also observe a decrease in the working-mode efficiency and the hysteresis effect. The above effects were observed explicitly for the values of beam misalignment starting from 1/4–1/3 of the wavelength. The axial misalignment of the electron beam can explain a certain mismatch between the experimental data and the results of numerical simulation with no allowance for this factor. It should be noted that in this work, we did not consider the effects related to azimuthal inhomogeneity and asymmetrical emission of the electron beam [18]. Allowence for these effects can explain the experimental results with greater accuracy.

REFERENCES

1. G. S. Nusinovich, *Radiotekh. Élektron.*, **19**, No. 8, 1788 (1974).
2. T. Idehara, K. Shibutani, H. Nojima, et al., *Int. J. Infrared and Millimeter Waves* **1**, No. 19, 1303 (1998).
3. O. Dumbrajs, *Int. J. Infrared and Millimeter Waves*, **15**, No. 7, 1255 (1994).
4. N. S. Ginzburg, G. S. Nusinovich, and N. A. Zavolsky, *Int. J. Electronics*, **61**, No. 6, 881 (1986).
5. M. A. Moiseev, L. L. Nemirovskaya, V. E. Zapevalov, and N. A. Zavolsky, *Int. J. Infrared and Millimeter Waves*, **18**, No. 11, 2117 (1997).
6. V. E. Myasnikov, M. V. Agapova, V. N. Ilyin, et al., *Radiotekhnika*, No. 2, 67 (2000).
7. A. G. Litvak, G. G. Denisov, V. E. Myasnikov, et al., in: *The 35th Int. Conf. on Infrared, Millimeter and Terahertz Waves, 2010, 4–10 Sept, Roma, Italy: Conference Digest*, P. Tu-E11.
8. V. E. Zapevalov, G. G. Denisov, V. A. Flyagin, et al., *Fusion Engineering and Design*, **53**, Nos. 1–4, 377 (2000).
9. V. E. Zapevalov, V. K. Lygin, O. V. Malygin, et al., *Radiophys. Quantum Electron.*, **50**, No. 6, 420 (2007).
10. T. Saito, T. Nakano, H. Hoshizuki, et al., *Int. J. Infrared and Millimeter Waves*, **28**, 1063 (2007).
11. N. A. Zavolskiy, V. E. Zapevalov, O. V. Malygin, et al., *Radiophys. Quantum Electron.*, **52**, Nos. 5–6, 379 (2009).
12. V. E. Zapevalov, N. A. Zavolskiy, O. E. Malygin, et al., *Radiophys. Quantum Electron.*, **52**, No. 12, 878 (2009).
13. V. E. Zapevalov, S. Yu. Kornishin, A. V. Kotov, et al., *Radiophys. Quantum Electron.*, **53**, No. 4, 229 (2010).
14. N. P. Venediktov, V. V. Dubrov, V. E. Zapevalov, et al., *Radiophys. Quantum Electron.*, **53**, No. 4, 237 (2010).

15. G. S. Nusinovich, *Introduction to the Physics of Gyrotrons*, Johns Hopkins Univ. Press, Baltimore, London (2004).
16. M. I. Rabinovich, *Radiophys. Quantum Electron.*, **8**, 566 (1965).
17. A. H. Nayfeh, *Introduction to Perturbation Techniques*, Wiley, New York (1984).
18. G. S. Nusinovich, A. N. Vlasov, M. Botton, et al., *Phys. Plasmas*, **8**, No. 7, 3473 (2001).